

J. Serb. Chem. Soc. 69 (12) 1129-1144 (2004)
JSCS-3239

UDC 519.87:547.422.22-31:661.183
Original scientific paper

Modeling of adsorber/desorber/catalytic reactor system for ethylene oxide removal

ZORANA L.J. ARSENIJEVIĆ,^{1,*} ŽELJKO B. GRBAVČIĆ² and BOŠKO V. GRBIĆ¹

¹*Institute for Chemistry, Technology and Metallurgy, University of Belgrade, Njegoševa 12, 11000 Belgrade and* ²*Faculty of Technology and Metallurgy, University of Belgrade, Karnegijeva 4, 11000 Belgrade, Serbia and Montenegro*

(Received 16 March 2004)

Abstract: The removal of ethylene oxide (EtO) in a combined system adsorber/desorber/catalytic reactor has been investigated. The combined system was a modified draft tube spouted bed reactor loaded with Pt/Al₂O₃ catalyst. The annular region was divided into two sections, the "hot" section contained about 7 % of catalyst and it behaved as a desorber and catalytic incinerator, while the "cold" section, with the rest of the catalyst, behaved as a sorber. The catalyst particles were circulated between the two sections by use of a draft tube riser. The Computational Fluid Dynamics (CFD) program package FLUENT was used for simulations of the operation of the combined system. In addition, a one-dimensional numerical model for the operation of the packed bed reactor was compared with the corresponding FLUENT calculations. The results of the FLUENT simulations are in very good agreement with the experimental observations, as well as with the results of the one-dimensional numerical simulations.

Keywords: draft tube spouted bed, Pt/Al₂O₃ catalyst, ethylene oxide removal, adsorber/desorber/catalytic reactor, numerical modeling, CFD modeling.

INTRODUCTION

The removal of ethylene oxide (EtO) from numerous emission sources (EtO production plants, manufacture of ethylene glycol, polymers, surfactants, food and pharmaceutical sterilizin units) is very important due to its mutagenic, teratogenic and cancerogenic effect on human health. Generally, it is considered that exposure to EtO at any level is harmful to health. Note that in most countries the EtO emission limit is 5 mg/m³ (2.55 x 10⁻⁴ vol.%).

Different technologies can be used to treat EtO emissions: wet scrubbers, thermal oxidizers, catalytic oxidizers and dry-bed reactors. Wet-scrubbers absorb EtO into a recirculating water-acid solution, converting the EtO to ethylene glycol. When the acid solution becomes saturated with ethylene glycol, it is transferred into a waste

* Author to whom correspondence should be addressed.

treatment device. Thermal oxidizers operate by oxidizing or burning EtO to form the products carbon dioxide, water vapor and heat. Thermal oxidizers require additional fuel. Catalytic oxidizers operate with the same end result as thermal oxidizers but at a lower temperature. Dry-bed reactors eliminate EtO by causing it to bind permanently to a reactant. They operate at ambient temperature. The appropriateness of the previous technologies for a specific process depends on several factors, such as: efficiency, energy consumption, secondary pollution, capital investments, *etc.* The principal advantages of catalytic oxidation are the high efficiency of the process, lower energy consumption than thermal oxidizers and absence of secondary pollution (NO_x or liquid or solid waste). Supported noble catalysts are widely used for the catalytic oxidation of organic vapors, particularly platinum, because of its high selectivity, resistance to poisoning and low ignition temperature.

In our previous work,¹⁻⁴ the results of EtO deep oxidation over Pt/Al₂O₃ catalyst in a packed bed reactor on the pilot scale (reactor diameter 315 mm) are presented, as well as a mathematical model that predicts the concentration and temperature profiles along the reactor fairly well. The main conclusion drawn from the packed bed investigations is that the conversion reached over 99.9 % when the inlet temperature of the reaction mixture was higher than 180 °C. With a relatively high EtO concentration at the inlet, the reactor could operate autothermally by use of an appropriate heat exchanger, since the heat of combustion is sufficient for preheating the inlet gas mixture to the ignition temperature. This would mean that external heating is necessary only during the start-up period. Note that the EtO inlet concentration should be a maximum of 30 % of the LEL (lower explosion limit) due to safety requirements. The LEL for EtO is 3 vol.%. Our experiments showed that the optimum catalytic oxidation parameters are: space velocity 17000 h⁻¹, inlet temperature of the reaction mixture 200 °C and an inlet EtO concentration 0.82 vol.%. Under these conditions, the exit gas temperature is 550 °C.

With lower inlet EtO concentrations, the process efficiency with the respect to the energy consumption decreases, since additional heat must be supplied in order to maintain the inlet gas mixture at 200 °C. Therefore, the treatment of emissions with low EtO concentrations is a high-energy consuming process.

The experiments conducted with a lower temperature of the inlet gas mixture (90–150 °C) showed that significant adsorption of EtO on the catalyst occurs.⁵ In this temperature region, the measured overall conversion arises from two simultaneous processes. A portion of the overall conversion is the consequence of “real” conversion due to surface reaction and the rest is the consequence of EtO adsorption on the catalyst. The presence of sorbed EtO on the catalyst was confirmed by the following: after completion of the operation in the lower temperature region (90 – 150 °C) the EtO feed was turned-off and the inlet temperature was increased above 180 °C. This caused an uncontrolled temperature rise along the catalyst bed as a consequence of the incineration of the previously sorbed EtO.

The ability of Pt/Al₂O₃ catalyst to bind EtO at significantly lower temperatures (90 °C) than the light-off temperature (180 °C), suggests that a cost-effective control method for the treatment of a large volume of dilute EtO streams is feasible and would involve a combination of adsorption, desorption and catalytic oxidation.

Some performances of a novel type of a combined system adsorber/desorber/catalytic reactor have already been published elsewhere⁵ and within this paper the investigations are expanded with a one-dimensional numerical modeling of the adsorption and reaction zone along with modeling by the Computational Fluid Dynamics (CFD) software FLUENT.

EXPERIMENTAL

Modified spouted bed with a draft tube reactor

The combined system is essentially a modified draft tube spouted bed (MDTSB) where the annular section of the bed is divided into two zones – adsorption (“cold”) zone and desorption and catalytic oxidation (“hot”) zone. The catalyst particles permanently or periodically circulate between the two zones through a draft tube riser. A schematic diagram of the proposed system is shown in Fig. 1.

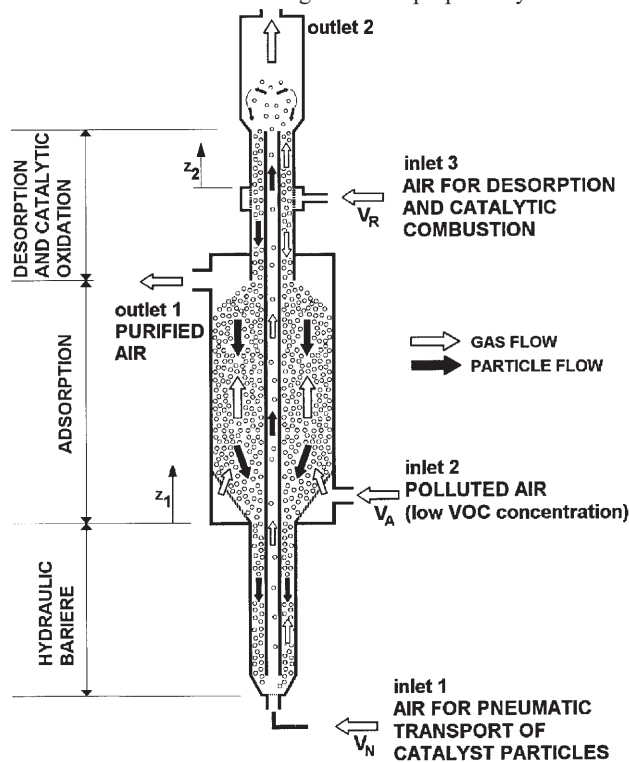


Fig. 1. Schematic diagram of the draft tube spouted bed adsorber/desorber/catalytic reactor (MSBDT).

A schematic diagram of the experimental system is given in Fig. 2. The annulus of the stainless steel reactor (1) loaded with 6.2 kg of Pt/Al₂O₃ (2) catalyst was divided into two sections: a reaction

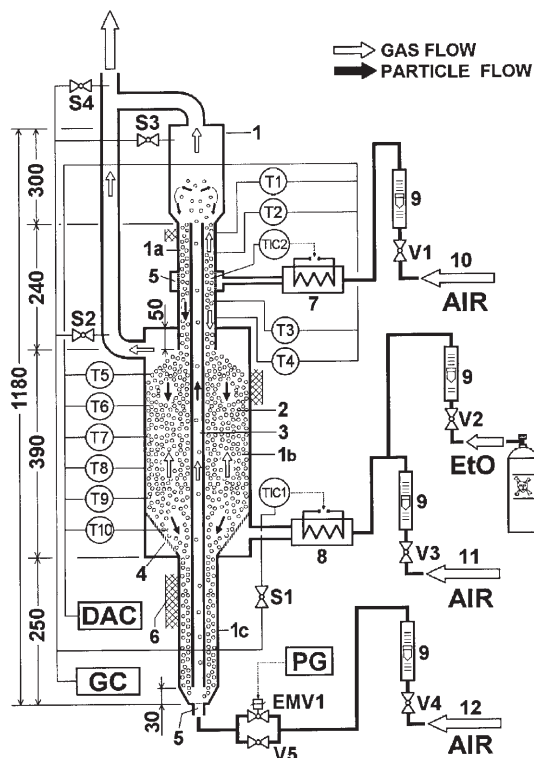


Fig. 2. Schematic diagram of the experimental system (1—column; 1a—annular section—adsorption and catalytic oxidation zone; 1b—annular section—desorption zone; 1c—extended annular section, hydraulic barrier for preventing EtO by-pass through the draft tube, from inlet 2 to outlet 2; 2—catalyst; 3—draft tube riser; 4—perforated cone $\Phi 1$ mm; 5—screen; 6—thermoisolation; 7—air heater (desorption and catalytic oxidation zone); 8—air heater (adsorption zone); 9—rotameters; 10—air for desorption and catalytic oxidation; 11—polluted air; 12—air for pneumatic transport of catalyst particles; EMV1—electromagnetic valve; V1–V4—valves; S1–S4—sampling valves; TIC1, TIC2 – thermo controllers; T1 – T10 –thermocouples; DAC—data acquisition system; GC—gas chromatograph; PG—programmator; (control of electromagnetic valve EMV1)

section (1a) with a height of 24 cm and a diameter of 6.5 cm and an adsorption section, which consist of a cylindrical part (1b), with a height of 39 cm and a diameter of 20 cm and a perforated conical part (4) with height of 10 cm followed by a narrow cylindrical part (1c). A draft tube riser (3) with a diameter of 1.8 cm, placed in the center of the reactor enable the circulation of the catalyst through both the sections. Transport of the catalyst from the bottom of the adsorption section to the top of the reaction section through the draft tube was attained by air flow (12). Two modes of catalyst transport were possible: continuous and pulse mode. In the pulse mode there was periodical circulation of the catalyst by means of an electromagnetic valve (EMV1) (active cycle). During the circulation of the catalyst, the air flow (12) was $14 \text{ Nm}^3/\text{h}$. Since a draft tube riser operates in an accelerating flow regime, this air flowrate for stable transport was determined using a model described in detail in a previous paper.⁷ When the catalyst is immovable (passive cycle), the air flow (12) was adjusted to $2 \text{ Nm}^3/\text{h}$ by a by-pass valve (V5). The role of this small flowrate and narrow cylindrical part of the annulus (1c) is to avoid flow of the reaction mixture through the draft tube. The superficial gas velocity (at 0°C) in the draft tube during the circulation period was about 63 % higher than the terminal velocity of a single particle. The catalyst circulation rate, measured at room temperature, was 0.019

kg/s. An air flow (11) of 30 Nm³/h was introduced into the annulus region through a perforated cone (4). This flowrate was used for the preparation of the reaction mixture with EtO and served as a heating medium for the annulus in the adsorption section. The introduction of EtO into the air flow (11) began when the desired temperature in the sorber had been achieved by means of an electric heater (8). The superficial gas velocity (at 0 °C) in the adsorption zone was about 27 % of the minimum fluidization velocity so that the annular region behaves as a moving packed bed during catalyst circulation. An air flow (10) of 2.9 Nm³/h that was passed through an electric heater (7) served to increase the temperature of the reaction section (1a) above the ignition point. The reaction section contained about 7 % of the total amount of the catalyst. Since the gas pressures at the top of the draft tube and at the top of the adsorption zone did not differ significantly, it is believed that approximately one half of the air flow (10) flows upside of the reaction section, while the other half flows downside. Under such assumption, the superficial gas velocity in the reaction section (at 0 °C) is 0.12 m/s which corresponds to a space velocity of 4837 h⁻¹.

There were ten NiCr–Ni thermocouples (T1–T10) placed along the reactor. All these temperatures were continuously registered by the data acquisition system (DAC). The valves (S1–S4) provided sampling for gas chromatographic (GC) analysis of the EtO inlet and outlet concentrations. The EtO inlet concentration was varied from 0.03 to 0.1 vol.%.

Catalyst

The Pt/Al₂O₃ catalyst was synthesized by dry impregnation of a spherical-shaped Al₂O₃ support with an aqueous solution of chloroplatinic acid.² The dried catalyst was reduced in a dynamic hydrogen–nitrogen mixture at a programmed temperature increase of 2 °C/min up to 500 °C. The key features of the catalyst are summarized in Table I.

TABLE I. Catalyst characteristics

Mean diameter	3.3 mm	Porosity	66 %
Surface area	96 m ² /g	Pt loading	0.12 wt.%
Density	3329 kg/m ³	Pt dispersion	86 %
Apparent density	1300 kg/m ³	Pt distribution	Egg shell
Pore volume	0.58 m ³ /kg	Width of Pt band	Approx. 100 μm

Reactor model

A one-dimensional reactor model^{1,4} neglecting the limitations of internal pore diffusion can be formulated by considering the mass and energy balance over an increment of the catalyst bed:

Mass balance. Reactant consumed at the catalyst surface due to the chemical reaction:

$$W_f = \frac{dy}{dz} = (1-\varepsilon_a)\rho_p r_A = (1-\varepsilon_a)\rho_p k y_p \tag{1}$$

Reactant transferred from the bulk flow to the catalyst surface:

$$W_f = \frac{dy}{dz} = k_m a_p \rho_f (y - y_p) \tag{2}$$

Energy balance. Heat generated in the solid phase due to the chemical reaction:

$$W_f C_p = \frac{dT_f}{dz} = (1-\varepsilon_a)\rho_p (-\Delta H_r) r_A = (1-\varepsilon_a)\rho_p (-\Delta H_r) k y_p \tag{3}$$

Heat transferred from the catalyst into the gas phase:

$$W_f C_p \frac{dT_f}{dz} = h_p a_p (T_p - T_f) \tag{4}$$

a_p represents the outer surface area of the particles per unit bed volume.

$$a_p = 6(1 - \varepsilon_a)/d_p \quad (5)$$

By combing Eqs. (1) and (2), the ratio (mass fraction of the reactant in the fluid just above catalyst surface)/(mass fraction of the reactant in the bulk flow) is given by:

$$\frac{y_p}{y} = \frac{1}{1 + k_p d_p / 6k_m \rho_f} \quad (6)$$

Note that for $y_p/y \rightarrow 1$ the overall process is controlled by the reaction kinetics, while for $y_p/y \rightarrow 0$ the overall process is controlled by the mass transfer.

The heat and mass transfer coefficients were evaluated using the Handley and Heggs⁸ correlation:

$$j_H = j_D = \frac{0.255}{\varepsilon_a Re_p^{1/3}} \quad (7)$$

where

$$Nu_p = \frac{h_p d_p}{\lambda} = j_H Re_p Pr^{1/3} \quad (8)$$

and

$$Sh_p = \frac{k_m d_p}{D} = j_D Re_p Sc^{1/3} \quad (9)$$

A kinetic investigation³ showed that the reaction of EtO oxidation is first order with respect to the EtO concentration with the following kinetic parameters $A = 584.83 \text{ kg}_{\text{air+ETO}}/\text{kg}_{\text{cat}} \text{ s}$ and $E = 41.67 \text{ kJ/mol}$. The above set of equations can be numerically solved in order to obtain the variation of conversion, bulk reactant concentration, surface reactant concentration, fluid temperature and particle temperature with bed height. The initial conditions are as follows: $y = y_0$, $T_f = T_{f0}$ and $T_p = T_{p0} = T_{f0}$ at the bottom of the bed. Note that in the adsorption zone the bed height was measured from the bottom of the cone (z_1 , Fig. 1). For the reaction zone it was assumed that one half of the reaction mixture is flowing downwards while one half is flowing upwards due to the symmetrical configuration. In the calculations, only the upper part was considered and the bed height was measured from the end of the radial inlet (z_2 , Fig. 1).

The CFD software "Fluent"

The Computational Fluid Dynamics (CFD) program package FLUENT⁹ (v4.48, 1997) was used for partial two-dimensional simulations of the operation of the combined system. The main scope was visualization of the process. CFD programs are generally limited by the available computational resources. Since our system is very complex, with 5 external and 5 internal inlets and outlets, FLUENT was used for partial two-dimensional simulations of the reaction and adsorption parts, separately, in order to obtain flow patterns, temperature and concentration fields.

RESULTS AND DISCUSSION

The MSBDT reactor operation is based on the adsorption of EtO in the adsorption zone, transfer through a draft tube riser to the reaction zone where the desorption and reaction of deep EtO oxidation occurs, after which the catalyst surface is "clean" and ready for the next cycle. The necessary condition for the efficient operation of the device is the provision of an adequate temperature for adsorption in the wider

part of the annulus. Therefore, at the beginning of the experiment, the adsorption zone of the catalyst was always heated up to at least 95 °C. Simultaneously, the reaction zone was heated up to 200 °C. Introduction of the EtO started after the required temperature profile along the reactor had been established.

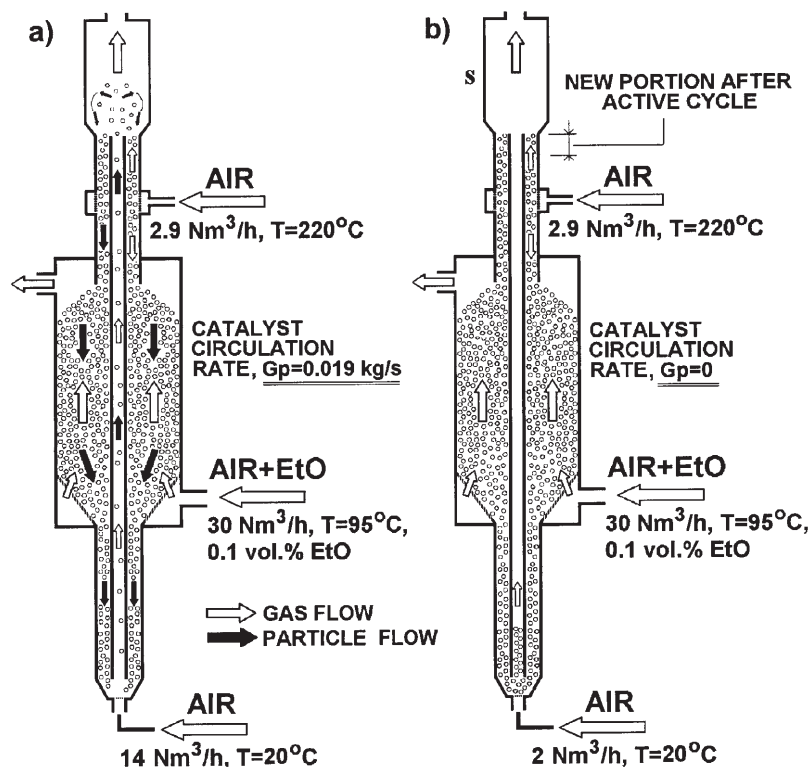


Fig. 3. Schematic diagram of MSBDT operation: a) active cycle (circulation on), b) passive cycle (circulation off).

Bearing in mind that in the reaction section several consecutive steps should occur: heating up of the catalyst; desorption of EtO derivatives; transport of the desorbed products through the pores to the outer shell of the pellet and surface reaction on platinum; a sufficient residence time of the catalyst in the reaction zone had to be set up. Continuous recirculation of the catalyst did not provide proper operating conditions since the residence time of the catalyst in the reaction section of about 25 s was too short for the catalyst particles to be heated up to the light-off temperature (200 °C). Note that catalyst particles coming into the reaction section from the draft tube have a temperature of about 100 °C. Under these conditions, the reaction was often transferred to the adsorption section without control. The problem was overcome by switching the draft tube riser to operate in the pulse mode. A schematic diagram of the MSBDT operation in one of the representative runs is given in Fig. 3. In this run, the inlet EtO concentration was 0.1 vol.% which corresponds to an EtO mass flowrate into the adsorption section of 0.06521 kg/h,

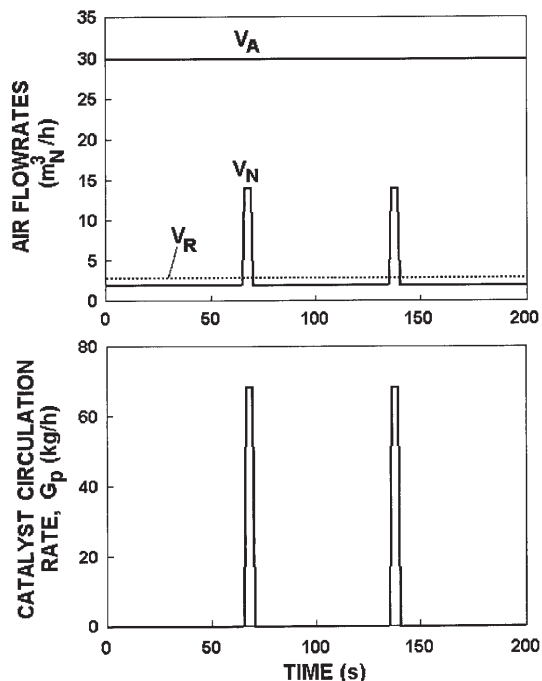


Fig. 4. Air flowrates and catalyst particle circulation rate.

the draft tube riser was active for 4 seconds, while the duration of the passive cycle was 65 seconds. For the same run, Fig. 4 gives the air flowrates and catalyst circulation rate as a function of the time, for the selected mode of operation. The duration of the active mode of the tube raiser was estimated according to catalyst mass flowrate and the volume of reaction section, considering also the quantity of EtO sorbed on the catalyst, as well as the expected temperature increase during incineration. Since the effective catalyst mass flowrate is $0.019 \text{ kg/s} \cdot (4 \text{ s} / (4 \text{ s} + 65 \text{ s})) = 0.0011 \text{ kg/s}$, a maximum quantity of sorbed EtO of $14.9 \text{ g}_{\text{EtO}}/\text{kg}_{\text{cat}}$ is expected. From the volume of the reaction section and the effective mass flowrate of the catalyst, it follows that after each active cycle, about 14 % of the catalyst in the reaction section had been replaced.

The corresponding temperature profiles along the MSBDT reactor prior to the introduction of EtO and in the steady state conditions of catalytic incineration are presented in Fig. 5a. In order to start the catalytic incineration of the adsorbed EtO, it was sufficient to provide a light-off temperature only in the thin layer (T3) of the reaction zone. Obviously, all the temperatures in the reaction zone in Fig. 5b were increased due to the catalytic incineration of EtO. The maximum temperature rise occurs at the point T2, where the temperature increased by over $300 \text{ }^\circ\text{C}$ with respect to the initial conditions (Fig. 5a). The temperature oscillations in the reaction zone are the consequences of the pulse mode of operation and are the most pronounced for T1. The temperature maximums coincide with the beginning of the supply of a new portion of the catalyst, whereas the minimums correspond to the

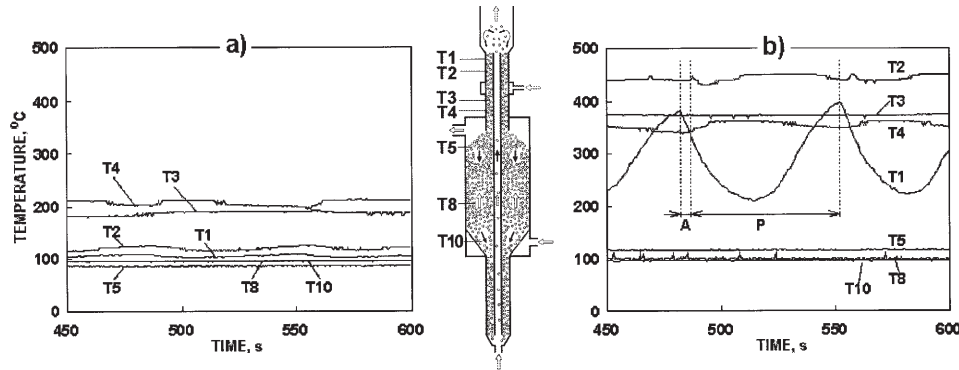


Fig. 5. Temperature profile along the MSBDT reactor: a) prior to the introduction of EtO, b) during catalytic EtO incineration ($c_{EtO} = 0.1 \text{ vol}\%$) A–active cycle, B–passive cycle.

beginning of the catalytic reaction during the passive period. The temperature rise of 20 to 40 °C that was noticed in the adsorption section is probably the consequence of two combined effects: the release of the heat of adsorption and the heat transferred from the reaction zone. In addition, it should not be forgotten that EtO oxidation at the catalyst surface can take place, contributing to the temperature rise in the adsorption zone. In the described run, the outlet EtO concentration was below the detection limit of the GC analysis.

The predictions of a one-dimensional model for the adsorption zone and for the reaction zone (run presented in Fig. 3) are given in Table II. In these calculations, the catalyst circulation was neglected since the active period (circulation on) consumes only 5.8 % of the total operating time. In the calculations, it was assumed that the catalyst temperature at the bottom of the bed is equal to the inlet air temperature. The model gives the axial variations of T_p , T_f , y , y_p and x_A . As can be seen, the overall conversion in the adsorption zone due to surface reaction is 39.34 % which corresponds to the rate of EtO removal by the surface reaction of 0.06251 kg/h. Since EtO was not detected at outlet 1 or the adsorption zone (Fig. 1), it can be concluded that the rest of the EtO (0.03792 kg/h) was adsorbed on the catalyst particles. The predicted temperature increase of about 18 °C along the adsorption zone agrees with the measured values (Fig. 5b), suggesting that the temperature rise in the adsorption zone mainly arises from the heat realized during EtO oxidation.

Calculations for the reaction section are only an approximation. Namely, the model assumes that the air flowing into the reactor contains EtO and that the catalyst is “clean”. In our case, however, the EtO is already bound on the catalyst and the air flowing into the reactor is “clean”. Assuming that these two situations are equivalent, the apparent EtO inlet concentration into the reaction zone is calculated from total EtO sorbed on the catalyst (0.03792 kg/h) and the air flowrate at the section inlet ($2.9 \text{ m}_N^2/\text{h}$). As can be seen, the calculated EtO inlet concentration flowing into the reaction section is 0.62 vol.%. Since the inlet EtO concentration to the

TABLE II. Model predictions for the adsorption section and for the reaction section (Note: z_1 and z_2 represents the axial coordinate measured from the bed bottom, see Fig. 1)

Adsorption section						
$V_0 = 30 \text{ m}_N^3/\text{h}$, $c_0 = 0.1 \text{ vol. \%}$, $T_{f0} = T_{s0} = 95 \text{ }^\circ\text{C}$, $H = 0.29 \text{ m}$, $SV = 3534 \text{ h}^{-1}$						
z_1	T_p	T_f	$y \times 10^3$	$y_p \times 10^3$	y_p/y	x_A
m	$^\circ\text{C}$	$^\circ\text{C}$	$\text{kg}_{\text{EtO}}/\text{kg}$	$\text{kg}_{\text{EtO}}/\text{kg}$	–	%
0.000	95.0	95.0	1.639	1.620	0.988	0.00
0.019	96.3	96.1	1.600	1.580	0.988	2.39
0.039	97.5	97.3	1.558	1.538	0.987	4.95
0.077	99.7	99.5	1.476	1.456	0.986	9.91
0.116	102.1	101.8	1.391	1.370	0.985	15.12
0.155	104.5	104.2	1.304	1.282	0.984	20.45
0.193	106.8	106.6	1.217	1.196	0.982	25.73
0.232	109.3	109.0	1.128	1.106	0.981	31.19
0.251	110.5	110.2	1.084	1.062	0.980	33.87
0.271	111.7	111.5	1.038	1.016	0.979	36.68
0.290	112.9	112.7	0.994	0.973	0.978	39.34
EtO mass flowrate into adsorption section, 0.06521 kg/h						
Amount of EtO removed by surface reaction, 0.06251 kg/h						
Amount of EtO removed by adsorption, 0.03792 kg/h						
z_2	T_p	T_f	$y \times 10^3$	$y_p \times 10^3$	y_p/y	x_A
V_m	$^\circ\text{C}$	$^\circ\text{C}$	$\text{kg}_{\text{EtO}}/\text{kg}$	$\text{kg}_{\text{EtO}}/\text{kg}$	–	%
Reaction section						
$V_0 = 1.45 \text{ m}_N^3/\text{h}$, $c_0 = 0.62 \text{ vol. \%}$, $T_{f0} = T_{s0} = 200 \text{ }^\circ\text{C}$, $H = 0.105 \text{ m}$, $SV = 4837 \text{ h}^{-1}$						
0.000	200.0	200.0	10.160	7.371	0.725	0.00
0.007	380.4	341.6	5.376	0.770	0.143	47.09
0.014	429.4	414.6	2.092	0.173	0.083	79.41
0.021	446.2	441.3	0.774	0.054	0.069	92.39
0.035	450.3	450.4	0.102	0.007	0.066	98.99
0.049	445.9	446.7	0.014	0.001	0.069	99.87
0.063	440.3	441.2	0.002	0.000	0.072	99.98
0.077	434.6	435.5	0.000	0.000	0.076	100.00
0.091	428.8	429.7	0.000	0.000	0.080	100.00
0.105	423.1	424.0	0.000	0.000	0.084	100.00

adsorption zone is 0.1 vol.%, it follows that the adsorption zone behaves essentially as a concentrator. With these assumptions, the calculations show that complete conversion occurs in reaction section after a very short distance from the inlet. The predicted temperature increase of about 220 °C along the reaction zone agrees fairly well with the measured values (Fig. 5b).

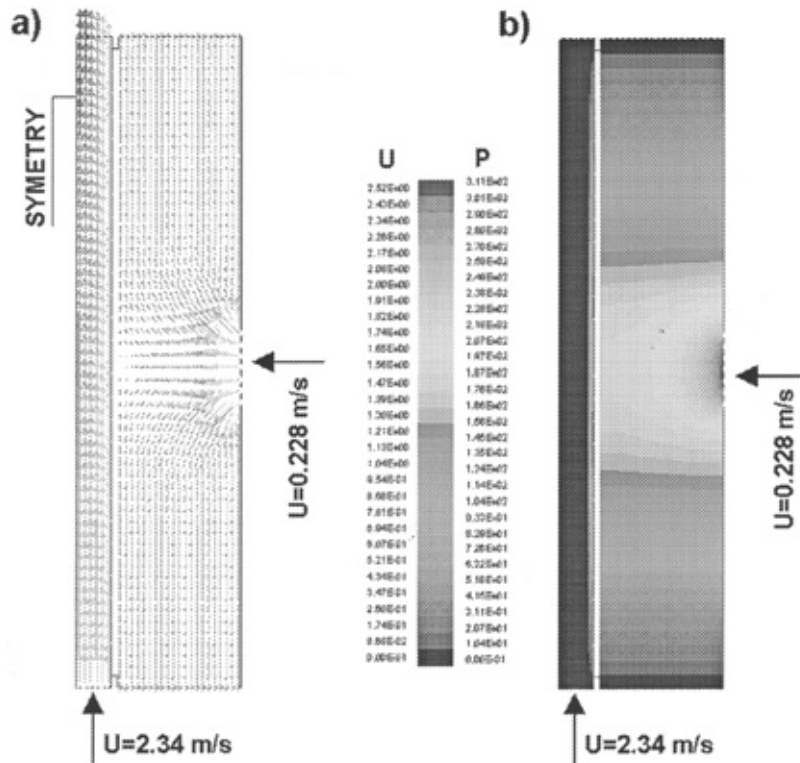


Fig. 6. FLUENT simulations in the reaction section; a) velocity vectors, b) static pressure field.

The one-dimensional model provides visualization of the reaction regimes through the combined system by means of the ratio y_p/y . As can be seen from Table II, in the adsorption zone, this ratio differs only slightly from one, indicating that the process is controlled by the kinetics of the surface reaction. Although in these considerations EtO adsorption was neglected, these values of the ratio y_p/y show that there are no external mass transfer limitations, regardless of the manner of EtO removal.

The sharp drop of the ratio y_p/y in the reaction section indicates that mass transfer governs the overall process. The model ascribes this drop to external mass transfer, but in our case the EtO consumed on the catalyst surface originated from the interior of the catalyst spheres. The EtO arrives at the sites by consecutive steps, desorption from the catalyst surface and transport through its pores. Obviously, these processes are significantly slower than the surface reaction, providing a good explanation for the necessity of employing the pulse mode, namely this mode ensures that the residence time is sufficiently long for the reaction to be completed.

The reaction section is defined in FLUENT as being two-dimensional with axis-symmetric geometry with a porous media and a chemical reaction active in the porous media only. Fig. 6a shows the velocity-vectors field, where the length and shading of the arrows representing the velocity magnitude. The static pressure field is shown in

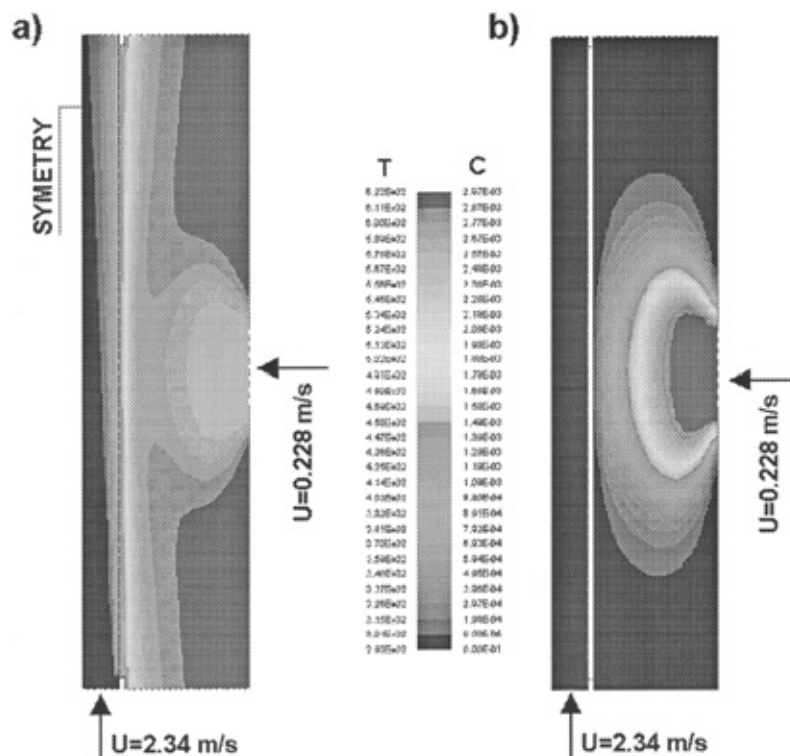


Fig. 7. FLUENT simulations in the reaction section; a) temperature field, b) concentration field.

Fig. 6b as a shade filled contour plot with the shading of domain presenting the magnitude of a selected variable according to the corresponding scale. The velocity and pressure profiles show that a uniform flow field is developed at a very short distance from the gas inlet. In addition, the orientation of the velocity-vectors confirm the assumption that approximately one half of the inlet air flow flows upside the reaction section, while the other half flows downside, due to the presence of the porous media. Fig. 7a illustrates the temperature field at the end of the passive cycle with a maximal temperature value of 420 °C, which is in good agreement with the experimental one. Fig. 7b shows the EtO concentration field *via* mass fractions. As can be seen, complete EtO combustion occurs within the region with the highest temperatures, *i.e.*, near the hot air introduction point. This means that EtO conversion is practically 100 %, which is in good agreement with the experimental observations and one-dimensional numeric simulations of the reaction section.

For an efficient operation of the combined system it is necessary to avoid reaction mixture flowrate through the draft tube, *i.e.*, polluted air flow from the inlet 1 to the outlet 2 (Fig. 1) should be avoided. This would mean that all of the inlet flow of polluted air must flow through the adsorption zone, *i.e.*, the velocity vectors in the narrow cylindrical part of the reactor (1c, Fig. 2) must be oriented upwards. As

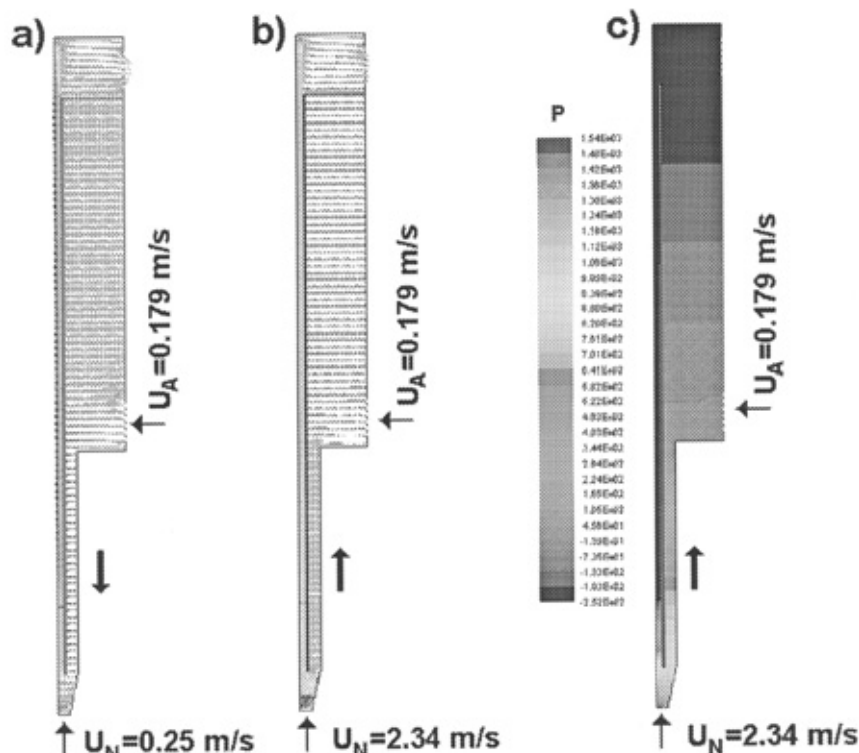


Fig. 8. FLUENT simulations of EtO “by-pass” prevention in the sorption section; a) velocity vectors $U_N = 0.25$ m/s; b) velocity vectors; $U_N = 2.34$ m/s; c) static pressure field, $U_N = 2.34$ m/s.

mentioned earlier, in our MSBDT reactor, by-pass is prevented by the small air flowrate through the nozzle at the bottom of the column (Fig. 2). This flowrate outside the catalyst recirculation period (passive cycle) was kept at $2 \text{ m}^3/\text{h}$, so that corresponding velocity at the nozzle was 2.34 m/s . We checked how accurately the minimum air flowrate for by-pass prevention can be predicted in this complicated flow and geometrical conditions using CFD software. The calculations were performed by fixing the velocity of the polluted air (inlet 2, Fig. 1) and varying the velocity at the nozzle for pneumatic transport of catalyst particles (inlet 1, Fig. 1). The results of the calculations are presented in Fig. 8. For an inlet velocity $U_N = 0.25 \text{ m/s}$ (Fig. 8a), the air flow in the lower part of the column is oriented downwards, so that under these conditions EtO by-pass can be expected. For an inlet nozzle velocity $U_N = 2.34 \text{ m/s}$ (Fig. 8b), the velocity vectors are oriented upwards so that EtO by-pass is prevented. The predicted conditions for the prevention of EtO by-pass agree quite well with the experimental observation. The static pressure field is shown in Fig. 8c for $U_N = 2.34 \text{ m/s}$, again as a shaded contour plot where the shading of a domain presents the magnitude of the selected variable according to the corresponding scale.

CONCLUSIONS

The investigations of EtO incineration over Pt/Al₂O₃ catalyst in a MSBDT reactor have shown that the system represents a cost-effective control method for the treatment of a large volume of dilute EtO streams. The advantages of the combined adsorber/desorber/catalytic reactor system with respect to a conventional packed bed catalytic reactor are reflected in energy savings. It is sufficient to heat the reaction mixture to the EtO adsorption temperature (about 100 °C) instead of heating to the ignition point (180–200 °C). The so-called adsorption zone has a twofold function, as a low-conversion catalytic reactor (less than 50 %) and as an EtO concentrator, since the concentration of desorbed EtO within the reaction zone is multiplied in comparison with the inlet concentration. Therefore, only a small part of the catalyst bed (about 7 %) has to be heated up to the ignition point in this system.

The results of FLUENT simulations are in very good agreement with the experimental observation, as well as with the results of one-dimensional numerical simulations. Generally, graphical displays of the FLUENT simulation results are useful for visualization of the process, while alphanumeric reports of local or averaged variable quantities in a selected plane or cross-section are necessary for quantitative post-processing analysis. FLUENT visualization, along with experimental observations and one-dimensional numeric simulations gives very useful information of the operation of the combined system.

Acknowledgment: The financial support of the Research Council of Serbia is gratefully acknowledged.

NOMENCLATURE

a_p	Outer surface area of the particles per unit volume, m ² /m ³
A	Pre-exponential factor, kg/kg _{cat} s
A_c	Cross-sectional area, m ²
C_p	Fluid heat capacity, kJ/kg °C
d_p	Particle diameter, m
D	Diffusivity of EtO in air, m ² /s
E	Activation energy, kJ/mol
H	Bed height, m
ΔH_r	Heat of reaction, kJ/kg
h_p	Heat transfer coefficient, kW/m ² °C
j_D	Mass transfer factor
j_H	Heat transfer factor
k	Rate constant, kg/kg _{cat} s
k_m	Mass transfer coefficient, m/s
Nu_p	Nusselt number ($= h_p D_p / \lambda$)
Pr	Prandtl number ($= \mu C_p / \lambda$)
r_A	Reaction rate, kg _A /kg _{cat} s
Re_p	Particle Reynolds number ($= d_p \rho_f U / \mu$)
Sc	Schmidt number ($= \mu \rho_f / D$)
Sh_p	Sherwood number ($= k_m d_p / D$)

SV	Space velocity, h^{-1}
T_f	Fluid temperature, $^{\circ}\text{C}$
T_p	Catalyst temperature, $^{\circ}\text{C}$
U	Superficial fluid velocity ($=V/A_c$), ms
V	Fluid flowrate, m^3/s
W_f	Mass flux of gas phase, $\text{kg}/\text{m}^2\text{s}$
x_A	Conversion
y	Mass fraction of the reactant in the fluid, kg/kg
y_p	Mass fraction of the reactant in the fluid just above the catalyst surface, kg/kg
z	Vertical coordinate, m
ε_a	Bed voids
μ	Viscosity of the fluid, Ns/m^2
λ	Thermal conductivity of the gas, $\text{kW}/\text{m}^{\circ}\text{C}$
ρ_f	Fluid density, kg/m^3
ρ_p	Particle density, kg/m^3

Subscripts

0	At the bed inlet ($z = 0$ and $z_1 = 0$ for the adsorption zone and $z_2 = 0$ for the reaction zone)
H	At the top of the bed
A	Adsorption section (inlet 2)
R	Reaction section (inlet 3)
N	Nozzle for pneumatic transport (inlet 1)

ИЗВОД

МОДЕЛОВАЊЕ СИСТЕМА АДСОРБЕР/ДЕСОРБЕР/КАТАЛИТИЧКИ
РЕАКТОР ЗА УКЛАЊАЊЕ ЕТИЛЕН ОКСИДА

ЗОРАНА Љ. АРСЕНИЈЕВИЋ,¹ ЖЕЉКО Б. ГРБАВЧИЋ² и БОШКО В. ГРБИЋ¹

¹Институт за хемију, технологију и металургију, Универзитет у Београду, Његошева 12, 11000 Београд
и ²Технолошко-металуршки факултет, Универзитет у Београду, Карнегијева 4, 11000 Београд

У комбинованом систему адсорбер/десорбер/каталитички реактор извршена су испитивања уклањања пара етилен оксида (ЕтО). У комбинованом систему је примењен модификовани фонтански слој $\text{Pt}/\text{Al}_2\text{O}_3$ катализатора са цевним уметком. Ануларни простор слоја катализатора се састоји из две зоне, "топле" зоне која садржи око 7 % укупне количине катализатора која има улогу десорбера и каталитичког конвертора, и "хладне" зоне која садржи преосталу количину катализатора и има улогу адсорбера. Циркулација катализатора између ове две зоне је омогућена пнеуматским транспортом кроз цевни уметак. Извршена је дводимензиона парцијална симулација коришћењем програмског пакета "FLUENT - Computational Fluid Dynamics Software" у циљу симулације одвијања процеса у појединим зонама комбинованог система. Једнодимензиони модел каталитичког реактора са пакованим слојем, искоришћен је за нумеричку симулацију реакционог дела комбинованог система, и ови резултати су упоређени са одговарајућим FLUENT-симулацијама. Добијено је веома добро слагање резултата FLUENT-симулација са експерименталним запажањима и једнодимензионим нумеричким симулацијама.

(Примљено 16. марта 2004)

REFERENCES

1. B. Grbić, Z. Grbavčić, Z. Saletić, A. Terlecki-Baričević, V. Jojić, *Proceedings the 2nd International Symposium and Exhibittion on Environmental Contamination in Central and Eastern Europe*, September 20–23, Budapest, 1994, p. 263
2. B. Grbić, V. Dondur, D. Jovanović, A. Terlecki-Baričević, *J. Serb. Chem. Soc.* **12** (1993) 1071
3. N. Radić, B. Grbić, Z. Jovanović, A. Terlecki-Baričević, Z. Arsenijević, *Proceedings of the 8th International Symposium on Heterogeneous Catalysis*, A. Andreev *et al.* (Eds.), Institute of Catalysis, Bulgarian Academy of Sciences, Sofia, October 5-9, Varna (1996) p. 377
4. B. Grbić, A. Terlecki-Baričević, Ž. Arsenijević, Z. Grbavčić, N. Radić, *Hem. Ind.* **49** (1995) 322
5. Z. Lj. Arsenijević, B. V. Grbić, Z. B. Grbavčić, N. D. Radić, A. V. Terlecki-Baričević, *Chem. Eng. Sci.* **54** (1999) 1519
6. O. Rentz, "Emissions of Volatile Organic Compounds (VOC) from Stationary Sources and Possibilities of their Control", *ECE VOC Task Force Report No 91-010*, Karlsruhe, 1990
7. Ž. B. Grbavčić, R. V. Garić, S. Dj. Jovanović, Lj. S. Rožić, *Powder Technol.* **94** (1997) 91
8. D. Handley, P. J. Heggs, *Trans. Inst. Chem. Eng.* **46** (1968) T251
9. FLUENT, Computational Fluid Dynamics Software (v4.48, 1997), Fluent inc., Lebanon, New Hampshire, USA.